

Behavior of Magnetorheological Fluid Composites Employing Carrier Fluids Certified for Landing Gear Use

Louise A. Ahur¹ and Norman M. Wereley²

Smart Structures Laboratory, Alfred Gessow Rotorcraft Center, University of Maryland, College Park, MD, 20742

Magnetorheological (MR) fluid composites were formulated in order to investigate their performance for potential use in landing gear hydraulic systems, such as shock struts. MR fluids prepared in this study utilized three hydraulic oils certified for use in landing gear as carrier fluids, two different average diameters of spherical magnetic particles, and a Lecithin surfactant. The fluids were characterized in order to measure and analyze their rheological behavior. Hence, different characteristics were considered, such as 1) magnetorheology as a function of magnetic field, 2) cycling of a small-scale damper undergoing sinusoidal excitations at frequencies of 2.5 and 5 Hz, and 3) impact testing for a range of magnetic field strengths and velocities using a free-flight drop tower facility. The goal of this research is to analyze the performance of these particular MR fluids, to compare their behavior to standard commercial MR fluids, and to determine their feasibility for use in helicopter landing gear.

Nomenclature

$\dot{\gamma}$	=	shear rate
C_{po}	=	postyield damping
C_{pr}	=	preyield damping
$f(t)$	=	nonlinear biviscous model
F_y	=	yield force
τ	=	shear stress
τ_y	=	yield stress
μ	=	post-yield viscosity
v	=	velocity
v_y	=	preyield velocity

I. Introduction

Magnetorheological (MR) fluids are suspensions of micron-sized magnetic particles, such as iron or cobalt, in a silicone or hydraulic oil carrier fluid.¹ Moreover, MR fluids have the ability to change properties when a magnetic field is applied and are used in an increasing range of applications, such as primary vehicle suspensions and semi-active vibration absorbing systems.² Yet, from published research, studies of MR fluids targeting applications including landing gear systems have not been widely investigated.³⁻⁵ During landing, an aircraft is subjected to a short duration impulsive impact, which is a critical factor in structural fatigue damage, crew and passenger discomfort, and dynamic stress. Consequently, several types of landing gear systems have been used in an attempt to reduce the touchdown impact. One prospective method is to use smart fluids such as MR fluids, whose advantage is to obtain continuously controllable rheological properties and fast response time to an applied magnetic field.^{6,7} Hence, new types of MR fluids were developed in this study, employing three different carrier hydraulic oils certified for landing gear use (MIL-H-5606, and MIL-PRF-83282 and MIL-PRF-87257). The fluid performance depended on characteristics such as 1) rheological properties with magnetic field off and on, 2) dynamic stiffness

¹Graduate Research Assistant, Aerospace Engineering, 3181 Martin Hall College Park MD 20742, Student (SS) #287192.

²Professor and Advisor, Department of Aerospace Engineering, 3181 Martin Hall College Park MD 20742, Associate Fellow (MC).

measurements using a small scale MR damper, and 3) dynamic axial impact testing with varying velocities and magnetic field strengths utilizing a drop tower facility. Consequently, this research investigates the effectiveness and feasibility of magnetorheological (MR) fluids employing fluids certified for landing gear use and compares their performance to commercial MR fluids for prospective use in landing gear systems.

II. Experiments and Methods

Three certified landing gear hydraulic oils were utilized as carrier fluids to prepare MR fluid composites: a mineral oil (MIL-H-5606) and two synthetic hydrocarbon oils (MIL-PRF-83282 and MIL-PRF-87257). The reason

for selecting these oils is to preserve important characteristics needed for landing gear systems, such as wide operational temperature ranges (-65 to 275°F), excellent anti-wear agents, and fire resistance properties.⁸

Each hydraulic fluid was then used to prepare two categories of MR fluid composites, depending on the average diameter of spherical iron particles present. The first

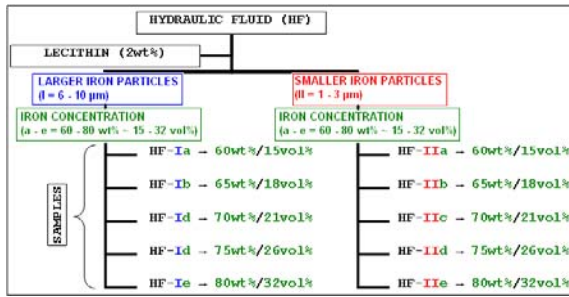


Figure 1. Fluid sample preparation and notation.

set contained iron particles of larger diameter (6 to 10 μm denoted by I), and the second set contained iron particles of smaller diameter (1 to 3 μm denoted by II). Also, lecithin powder was added as a surfactant to reduce agglomeration and mediate settling. In order to prepare stable MR fluids, a specific amount of hydraulic oil was mixed with 2 weight % (wt. %) of lecithin powder using a high speed shear mixer operating at 11,000 rpm. After consistently mixing for 30 minutes, iron particles were added in specific concentrations to each fluid and remixed for an additional hour. Accordingly, samples varying from 60 to 80 wt. % (15 to 32 vol. %) in iron particle concentration were produced, and each sample notation includes three important parts: the hydraulic oil used (e.g. 83282), iron particle size (I ≡ 6-10 μm or II ≡ 1-3 μm), and iron particle concentration (e.g. d for 75 wt. % iron), as presented in Fig. 1.

Magnetorheological characterization was performed on all of the MR fluid composites using a Paar Physica MCR 300 parallel disk rheometer shown in Fig. 2. First, neat hydraulic oils and the prepared MR fluids were tested singly in the rheometer to approximate their dynamic viscosity (shear stress versus shear rate in the absence of magnetic field). Then, the prepared samples were loaded onto the rheometer, which had a standard 1 mm gap separating the rotating disk from the platen. On-field testing was executed with increasing current from 0.2 to 2 A to obtain fluid flow curves and determine magnetic saturation of each sample.

For this study, the fluid flow curves were characterized using the Bingham Plastic (BP) model, which is a generalized model for relating the shear stress, τ , to shear rate, $\dot{\gamma}$, as a viscoplastic flow with a yield stress.¹ The equation for $\dot{\gamma} > 0$ is:

$$\tau = \tau_y + \mu \dot{\gamma} \quad [1]$$



Figure 2. Paar Physica MCR 300 parallel disk rheometer.

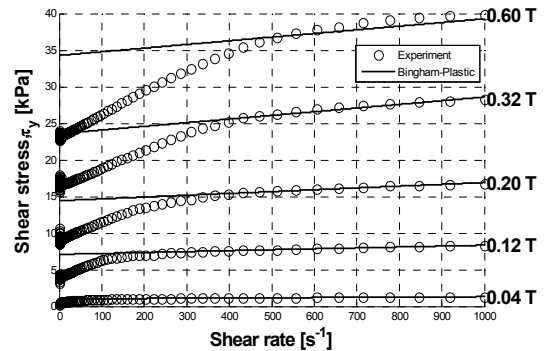


Figure 3. Typical MR fluid flow curves modeled with the Bingham Plastic Method (Commercial fluid MRF 126CD).

The Bingham Plastic model parameters are the yield stress, τ_y (in Pa) and the post-yield viscosity, μ (in Pa sec). τ_y is the intercept of the high shear rate asymptote with the shear stress axis, and μ is the slope of that asymptote. Typical flow curves fitted with the Bingham Plastic model are shown in Fig. 3. This model has also been used to model Poiseuille flow in electrorheological and magnetorheological dampers.^{6,9,10}

Dynamic stiffness of the MR fluid composites was determined by analyzing the behavior of a magnetorheological damper, containing the fluids and undergoing sinusoidal loading. Only MR fluids containing iron particle concentration of 80 wt. % (or 32 vol. %) were tested in the damper, whose behavior depended on amplitude and frequency of motion. In order to obtain a magnetic field inside the damper, electric current was used to trigger the magnetic circuit. The MR damper utilized was a modified Rheonetics SD-1000-2, manufactured by Lord Corporation and tested on an 810 Material Test System (MTS). A

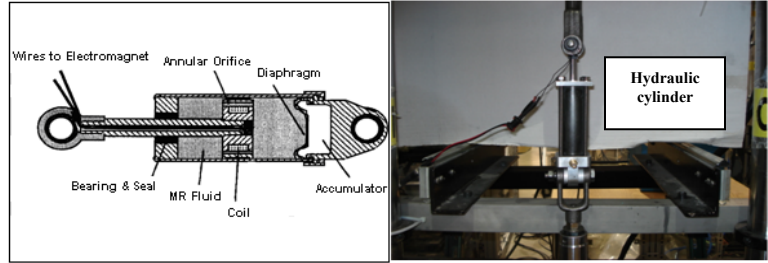


Figure 4. (a) Cross section of a Rheonetics SD-1000-2 MR damper from Lord Corporation; (b) Setup of a modified Rheonetics MR damper on MTS machine.

cross section of the damper and the test setup are shown in Fig. 4a and 4b. The damper hydraulic cylinder shown in Fig. 4b is technically 102 mm in length and 45 mm in diameter, and it encloses the damper piston, in which a magnetic circuit is mounted. Inside and at the base of the hydraulic cylinder, a nitrogen accumulator is used to pressurize the approximate 50 ml of MR fluid contained. The accumulator also helps prevent cavitation in the fluid at the low pressure side of the piston while in motion, discussed by Dyke et al. in Ref. 11.

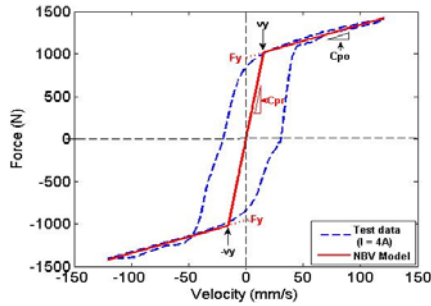


Figure 5. Typical MR damper test data modeled with the Nonlinear Biviscous (NBV) model.

MR fluid is plastic in the preyield and postyield regions, and the preyield damping, C_{pr} is greater than the postyield damping, C_{po} . The yield force, F_y in the damper model is represented by the high velocity asymptote intercept with the force axis as shown in Fig. 5. This model has been used to analyze leakage in electrorheological dampers in Refs. 15 and 16, and an advantage is that it accounts for the preyield damping part a of typical viscoplastic preyield behavior of MR fluids. Three piecewise equations are used to characterizing the Nonlinear Biviscous (NBV) model:

$$f(t) = \begin{cases} C_{po}v + F_y & v \geq v_y & [2] \\ C_{pr}v & -v_y \geq v \leq v_y & [3] \\ C_{po}v - F_y & v \leq -v_y & [4] \end{cases}$$

The preyield velocity is:

$$v_y = F_y / (C_{pr} - C_{po}) \quad [5]$$

Moreover, a free-flight drop test facility with a 59 kg drop carriage, as shown in Fig.7, was used at the University of Maryland to conduct dynamic axial crash tests on a MR damper enclosing synthetic oil-based MR fluid composite, containing 6 to 10 μm iron particles at a concentration of 80 wt. % (denoted mr83282-1e). Recently,

MR dampers have been highlighted as a promising candidate for crashworthiness systems, and several impact tests have been conducted.^{3,17,18,19} Therefore, the performance of one of the prepared landing gear oil-based MR fluid composite in a MR damper



Figure 7. Drop test carriage at the University of Maryland College Park.

subjected to drop testing is important to verify the tuning nature of the response of the device at different stroking velocities representative of helicopter landing impacts. The experiment instrumentation included a load cell located on a base plate as shown in Fig. 8, which was tightly attached to the ground, a LVDT fastened to the damper to monitor the displacement of the damper piston as a function of time, and a power supply to provide current necessary to generate a magnetic field in the damper. In addition, the raw signal from the sensor was filtered through a 2311 VISHAY signal conditioning amplifier and the data was transferred to a computer using a SCC-68 National Instruments data acquisition interface (which changed analog data to digital). Then, the data was exported to MATLAB compatible formats for analysis.

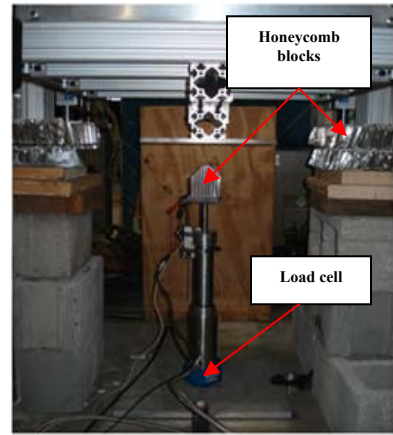


Figure 8. MR damper mounted for drop testing.

Testing of the MR fluid composite enclosed in the damper was achieved by positioning the damper vertically on the base plate. Then, a block of aluminum honeycomb measuring 90x60x60 mm was taped on a small plate, which was mounted on the top end of the damper. The purpose of using the aluminum honeycomb block was to prevent the ringing in the load cell due to metal-to-metal contact and reduce the inertial spike associated with the impact acceleration of the piston rod.²⁰ Additional larger honeycomb blocks were placed on top of cement bricks and wood blocks (on each side of the damper) to stop the carriage platform after about 3.8 cm of stroke, which needed to be less than the LVDT stroke of 4.6 cm to prevent damaging it.

Before each test, the MR damper rod was extended, and the drop carriage was raised to a specific height corresponding to a selected impact velocity. Then, the drop carriage was released to freely fall under gravity until impacting on the test assembly, and the load cell and LVDT data were recorded.

III. Results and Discussions

A. Rheology Results

Rheological tests were performed on all of the prepared MR fluids shown in table 1 at room temperature. A few challenges were encountered in testing. MR fluid composites tended to be ejected from the test area when testing low viscosity fluid at high shear rates, especially at low field strengths. Another difficulty was the inability for the samples to stay within the test area without a small magnetic field being applied. For each test, 0.3 ml volume was measured in the test area. Then, the fluid was sheared by the rotating top disk, as the bottom disk stayed stationary. The off-state viscosity (zero magnetic field strength) measurements were performed with the shear rate ranging from 10 to 1000 s^{-1} . The shear rate of the flow curves (magnetic field on), shown in Fig. 3, ranged from 0.1 to 1000 s^{-1} , with current increasing from 0.2 to 2 A in 0.2 A increments, and from 2.5 to 5 A in 0.5 A increments. The maximum shear rate was 1000 s^{-1} to prevent fluid from escaping the test area at higher RPM, and the maximum current was 5 A (corresponding to a magnetic flux density of about 1 Tesla). Flow curves were measured using the supplied US200 software compatible with the rheometer.

Table 1. MR fluid compositions.

Iron wt%	60	65	70	75	80
Fluids	(a)	(b)	(c)	(d)	(e)
MR Fluid with mineral oil	mr5606	X	mr5606	X	mr5606
MR Fluid with synthetic oil 1	mr83282	mr83282	mr83282	mr83282	mr83282
MR Fluid with synthetic oil 2	mr87257	mr87257	mr87257	mr87257	mr87257

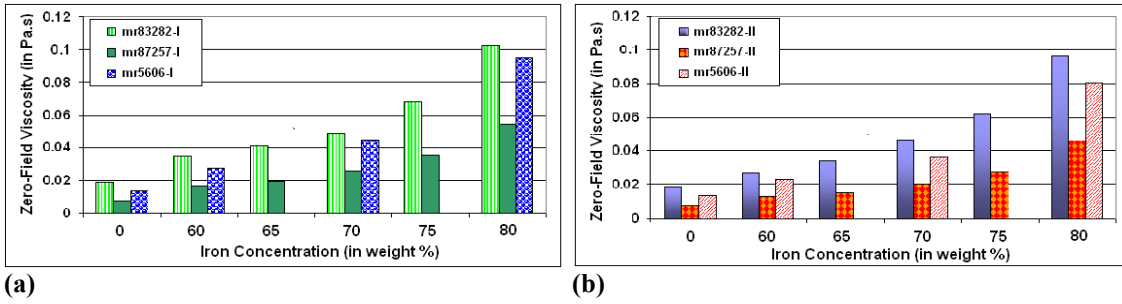


Figure 9. Zero-field viscosity of MR fluid composites as iron concentration increases. (a) 6-10 μm particle diameter. (b) 1-3 μm particle diameter.

Rheology of neat hydraulic oils showed that the viscosity of the synthetic oil MIL-PRF-87257 is the lowest when compared to the other oils. As iron particles (1 to 3 μm or 6 to 10 μm) were added to the oils, there was a proportional increase, but the viscosity pattern was conserved as illustrated in Fig. 9a and 9b. Indeed, while the iron concentration was increased, MR fluid composites containing the synthetic oil MIL-PRF-87257 had a 40% lower zero-field viscosity compared to the other fluids. Moreover, the viscosity of the MR fluids depended significantly on the choice of hydraulic oil and the iron particle concentration. For instance, each sample viscosity increased by more than 80% after adding 80 wt. % (or 32 vol. %) iron particles to the carrier fluids.

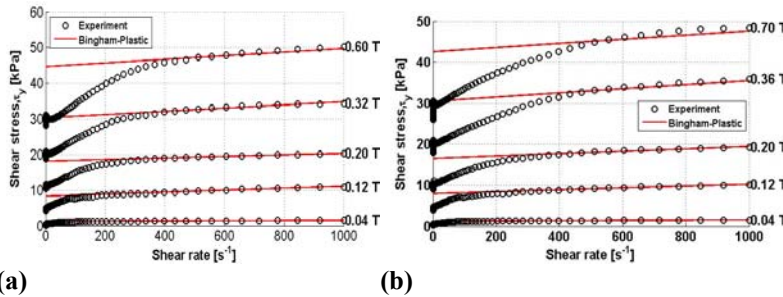


Figure 10. Selected and modeled (with Bingham Plastic) flow curves for MR fluid composites: (a) synthetic oil-based mr83282-Ie (80 wt % iron) and (b) mineral oil-based mr5606-Ie.

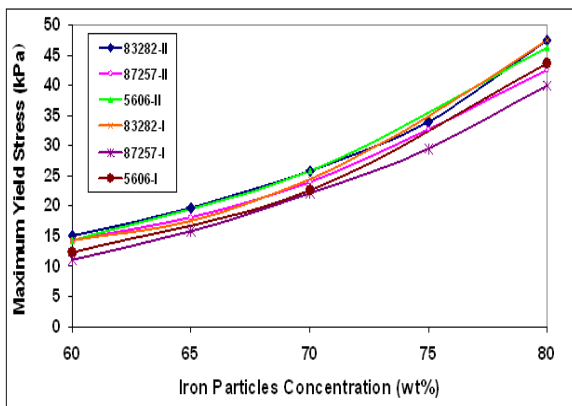


Figure 11. Maximum yield stress for all MR fluid composites as a function of iron particle concentration.

Flow curves of all samples were measured and modeled using the Bingham Plastic model, and Fig. 10a and 10b show selected flow curves modeled for MR fluid composites containing one of the synthetic oils (MIL-PRF-83282) and the mineral oil (MIL-H-5606). In addition, the maximum yield stress saturation of all MR fluid samples was determined and compared. As a result, it was observed that the performance of the fluids did not strongly depend on the choice of iron particle sizes or the type of carrier hydraulic oil, but it was significantly dependent on the iron particle concentration. As particle concentration increased, the maximum yield stress increased as well. The yield stress improved by more than 65% for all MR fluids containing smaller (1 to 3 μm) particles and about 70% for fluids with larger (6 to 10 μm) particles. The performance is illustrated in Fig. 11.

MR fluid rheology was compared with a commercial MR fluid from Lord Corporation (MRF126CD ~ 26 vol. % iron concentration). Synthetic oil-based fluid containing larger (6 to 10 μm) particles, at 75 wt. % (or 26 vol. %) iron concentration (referred as mr83282-I_d in table 1), had an off-state viscosity lower than the commercial MR fluid, as illustrated in Fig. 12a. In fact, it is important to keep the off-state viscosity low to prevent adding excessive weight to MR devices²¹ and to maintain high frequency vibration performance.²² Also, both fluid maximum yield stress performances followed similar trends, as Fig. 12b shows.

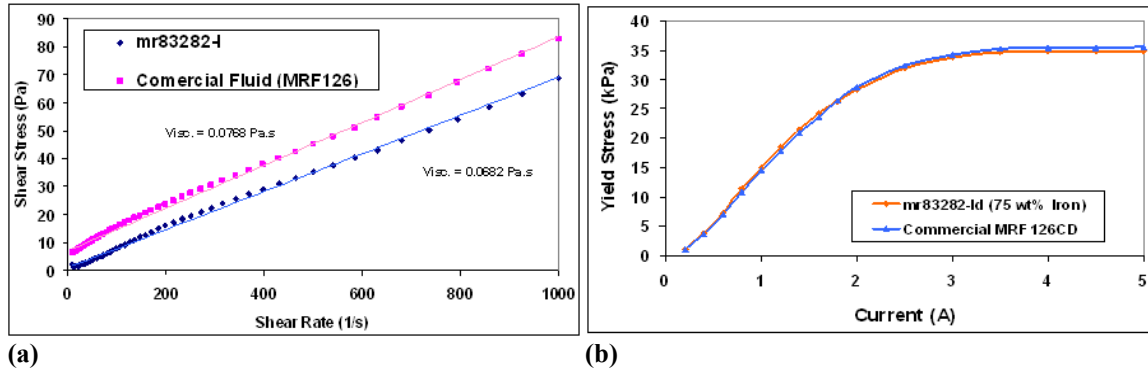


Figure 12. MR83282-Id performance compared to a commercial MR fluid. (a) Zero-field viscosity (b) yield stress (within 2%).

B. Damper Results

Hysteretic behavior of the linear stroke MR damper containing MR fluids was studied using high iron particle concentration fluids (80 wt. % or 32 vol. %). The damper was tested using different sinusoidal shaft displacements: 1.27, 2.54, 5.08, and 7.62 mm, at two frequencies (2.5 and 5Hz), while the magnetic field was controlled using a power supply. Current was applied from 0 to 4 A with 1 A increments to activate the damper electromagnet. The test matrix presented in table 2 was programmed using the software MTSTESWARE, which executed the inputs. The resulting force was measured by a load cell, mounted on the MTS-810 load frame.

Typical data shown in Fig. 13a and 13b are the force versus displacement and the force versus velocity, respectively, for current values of 0 to 4 A at 2.5Hz. As the applied current increased, so did the magnetic field; therefore, the damping, which is represented by the area enclosed by the force versus the displacement hysteresis cycle in Fig. 13a, also increased. The force versus velocity cycles in Fig. 13b show a behavior similar to a Bingham Plastic.^{6,23} When the damper restoring force was less or greater than the yield force, F_y , the damper operated in the preyield or the postyield region². Hence, the NBV method was used to characterize the MR effect (preyield and postyield regions). The model parameters (C_{pr} , C_{po} , F_y , and v_y) were identified from experimental data, and a MATLAB[®] routine was used to program a constrained least-mean-squared error minimization. Parameters were identified for all MR fluid composites containing one of the synthetic oils. Mr83282 fluids followed similar patterns,

Table 2. MR damper test matrix. Tests were executed at 2.5 and 5 Hz.

Current in A	Sinusoidal Shaft Displacement in mm			
	1.27	2.54	5.08	7.62
0	x	x	x	x
1	x	x	x	x
2	x	x	x	x
3	x	x	x	x
4	x	x	x	x

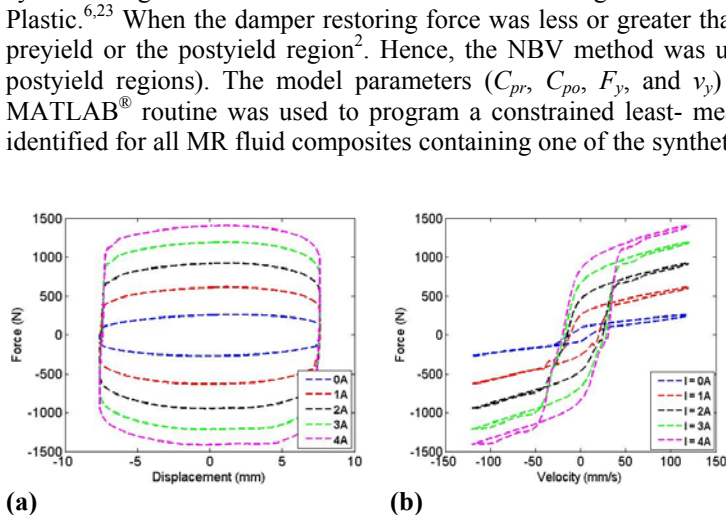


Figure 13. Hysteresis cycles of MR damper containing the commercial MR fluid. Sinusoidal excitation of 7.62 mm at 2.5 Hz. (a) Force (N) versus displacement (mm); (b) Force versus velocity (mm/s).

and their parameters are plotted versus the current in Fig. 14a through 14d. As noted earlier, the preyield damping, C_{pr} , is greater than the postyield damping, C_{po} , as current increases at both frequencies, shown in Fig. 14a and 14b. Furthermore, the preyield velocity became larger as the frequency increased. In addition, the yield force depended on the type of carrier fluid used. For instance, the yield force of all MR fluid composites containing the synthetic oil MIL-PRF-87257 was 27% lower than the yield force of MR fluids prepared with the other synthetic carrier fluid (MIL-PRF-83282).

MR fluids were tested in the damper to verify the nonlinear behavior as a

function of magnetic field. Figures 15a and 15b represent the force versus displacement and the force versus velocity of the MR fluid composite containing the synthetic oil MIL-PRF-87257 for current values of 1 and 4 A at 2.5 Hz. The NBV model was used to characterize the preyield and postyield damping, as well as the yield force of of

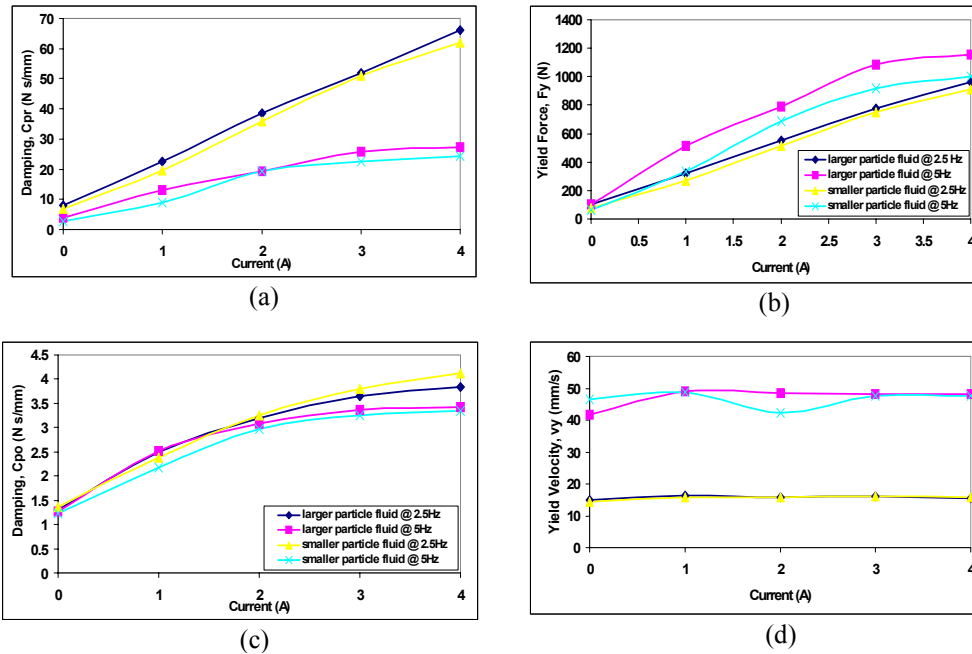


Figure 14. NBV model parameters (C_{pr} , C_{po} , v_y , and F_y) plotted versus applied current for mr83282 fluids. (a) preyield Damping, Ns/mm; (b) yield Force, N; (c) postyield Damping, Ns/mm; (d) preyield velocity, mm/s.

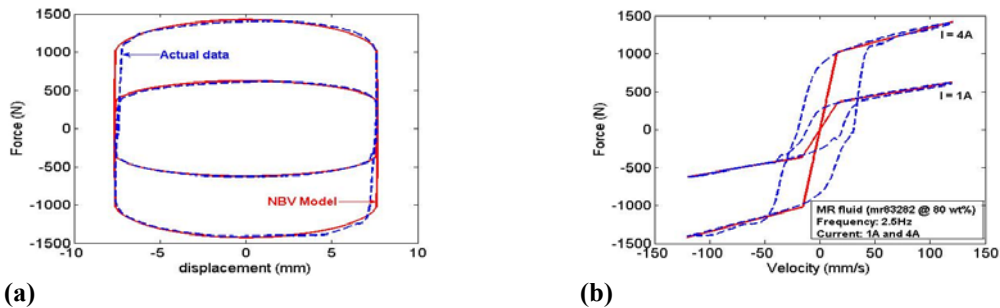


Figure 15. NBV model of MR fluids with synthetic oil (MIL-PRF-87257) as a carrier fluid (6-10 μm particles) at 2.5 Hz and currents of 1 and 4A. (a) Force versus displacement; (b) force versus velocity.

the MR damper. The NBV model accurately models the force versus displacement cycles, hence, the damping.

MR fluid composites (of 32 vol. % particle concentration) performance were compared with a commercial MR fluid from Lord Corporation (MRF132 of the same particle concentration). Yield forces of fluids containing synthetic oil MIL-PRF-83282 and mineral oil MIL-H-5606 with larger (6 to 10 μm) iron particles followed the same pattern as the yield force of the commercial fluid, particularly at 5Hz. Figure 16 illustrates the results, and all three fluid yield forces plotted versus the current show that the maximum yield forces are relatively close (within 5%).

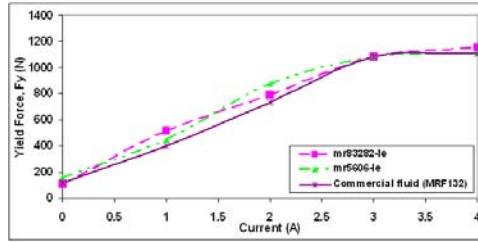


Figure 16. Yield force (N) versus current (A) for the synthetic oil (mr83282-Ie) and the mineral oil (mr5606-Ie) based MR fluid, and the commercial MR fluid (MRF132).

C. Drop Test Analysis

Table 3. Peak stroking force (N) for applied current and impact velocity.

Velocity (m/s)	Current (Amperes)		
	0	0.5	2
1.1	950	1360	3770
2.8	2940	3960	6880
4.1	7530	9080	10100

Synthetic hydraulic oil-based MR fluid composite with 6 to 10 μm iron particles at 80 wt. % concentration (denoted mr83282-Ie) was used inside the damper subjected to drop testing. This particular fluid was selected due to its favorable performance based on the rheological and damper test results. The software National Instruments executed the inputs and was exported to MATLAB through a routine to filter and plot the data. Hence, results of peak stroking force values for a corresponding range of impact velocities and applied magnetic

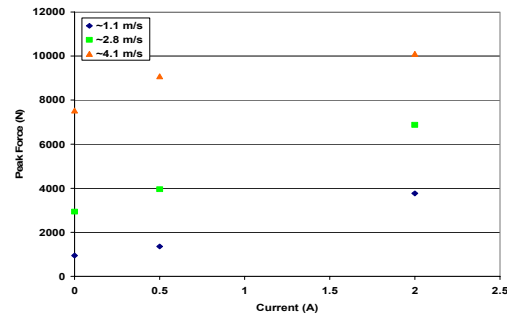
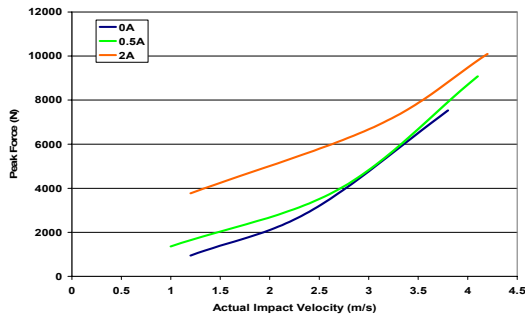


Figure 17. Peak stroke versus current and impact velocity. (a) Force versus velocity in m/s. (b) Force versus current in ampere.

field strengths were recorded and are shown in table 3. The peak force increased as the magnetic field and the impact velocity increased. In Fig. 17a, while the velocity increased, an increase in the peak stroking force was observed and was due to the viscosity related component of the shear stress. Also, in Fig. 17b, as the current, hence the magnetic field was augmented, there was an increase in the peak stroking force, which was attributed to the increase in the yield stress related component of the shear stress.²² Moreover, the ability to significantly tune the level of the stroking force was higher at lower impact velocity but slightly reduced as the velocity increased. The synthetic oil-based MR fluid composite (mr83282-Ie) used for the drop test showed tunable behavior as the magnetic field was changed. In fact, the peak stroking force changed as a function of time, and the energy generated by the MR damper altered as well, as observed in Fig. 18 for one specific impact velocity (of 2.8 m/s).

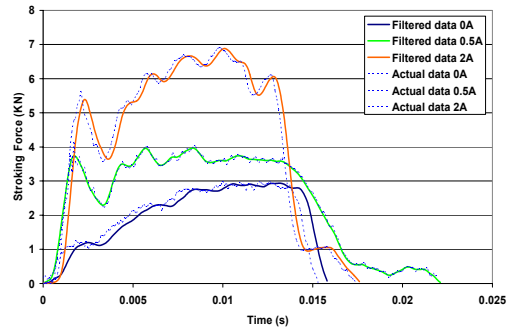


Figure 18. Stroking force versus time at impact velocity of 2.8 m/s.

IV. Conclusion

An analysis of the behavior of magnetorheological (MR) fluid composites, prepared using three different carrier hydraulic oils certified for landing gear use, was conducted, and the feasibility and effectiveness for prospective use in landing gear systems were assessed. First, magnetorheology was tested as a function of applied field, and the experimental data were characterized using the Bingham Plastic model. Using flow curve data, the yield stress and viscosity of the MR fluid composites were identified. The MR landing gear fluid composite compared favorably with a commercial MR fluid (both containing 26 vol. % magnetic particles). Then, the performance of a linear stroke MR damper, containing the MR fluids, was characterized using a Nonlinear Biviscous (NBV) model. The NBV model was used to successfully reconstruct the force versus displacement diagram and to identify the pre-and-post yield damping and yield force using the force versus velocity plots.

MR damper behavior was compared to a second commercial MR fluid (of 32 vol. % particle concentration). The yield forces of the MR fluid composites containing the larger (6 to 10 μm) iron particles (with 32 vol. % particles) compared favorably with the commercial fluid force, and their maximum yield forces remained within 5% of each other.

Last, synthetic oil-based MR fluid (containing 32 vol. % iron particles) was utilized in an MR damper and subjected to high shear rate drop testing to experimentally verify the tuning nature of the MR device at different the impact velocities and magnetic field strengths. Consequently, the peak stroking force and the energy dissipated by the MR damper strongly depended on the changes in the magnetic field strengths.

Different tests done to characterize these particular MR fluid rheological behaviors showed that typical landing gear hydraulic oils can be utilized to make suitable MR fluids.

Acknowledgments

Research support provided by the Center for Rotorcraft Innovation and the National Rotorcraft Technology Center, Aviation and Missile Research, Development and Engineering Center under Technology Investment Agreement with W911W6-06-2-0002. Additional research support provided under a contract from the U.S. Navy (Form Fit and Function Engineering as prime contractor).

References

- ¹Chaudhuri, A., Yoo J. H., John, S., and Wereley, N. M., "Bidisperse Magnetorheological Fluids using Fe Particles at Nanometer and Micron Scale," *Journal of Intelligent Material Systems and Structures*, Vol. 17, No. 5, 2006, pp. 393-400.
- ²Snyder, A., Kamath, G. M., and Wereley, N. M., "Characterization and Analysis of Magnetorheological Damper Behavior under Sinusoidal Loading," *AIAA J. Aircraft*, Vol. 39, No. 7, 2001, pp. 1241-1253.
- ³Choi, Y. T., and Wereley, N. M., "Vibration Control of a Landing Gear System Featuring ER/MR Fluids," *Journal of Aircraft*, Vol. 40, No. 3, 2003, pp.432-439.
- ⁴Batterbee, N. D., Stanway, R., and Wolejsza, Z., "Magnetorheological Landing Gear: 1. A Design Methodology," *Smart Materials and Structures*, Vol. 16, 2007, pp. 2429-2440.
- ⁵Batterbee, D. C., Sims, N. D., Stanway, R., and Rennison, M., "Magnetorheological Landing Gear: 2. Validation Using Experimental Data," *Smart Materials and Structures*, Vol. 16, 2007, pp. 2441-2452.
- ⁶Lee, H. G., Choi, S. B., Han, S. S., and Kim, J. H., "Bingham and Response Characteristics of ER Fluids in Shear and Flow Modes," *International Journal of Modern Physics B*, Vol. 15, No. 6 and 7, 2001, pp. 1017-1024.
- ⁷Carlson, J. D., Catanzarite, D. N., and St. Clair, K. A., "Commercial Magneto-Rheological Fluid Devices," *Proceedings of 5th International Conference on ER Fluids, MR Suspensions and Associated Technology*, World Scientific, Singapore, Republic of Singapore, 1996, pp. 20-28.
- ⁸Aviation Maintenance and Training Manual, "Hydraulic Contamination and Related Servicing/Test Equipment," *Integrated Publishing* [online database], Ch. 4, pp. 4-20, URL: http://www.tpub.com/content/aviation/14018/css/14018_178.htm [cited 13 Feb. 2008].
- ⁹Gavin, H. P., Hanson, R. D., and Filisko, F. E., "Electrorheological Dampers, Part I: Analysis and Design," *ASME Journal of Applied Mechanics*, Vol. 63, No. 3, 1996, pp. 669-675.
- ¹⁰Wereley, N. M., and Pang, L., "Nondimensional Analysis of Semi-Active Electrorheological and Magnetorheological Dampers Using Approximate Parallel Plate Models," *Smart Materials and Structures*, Vol. 7, No. 5, 1998, pp. 732-743.
- ¹¹Dyke, S. J., Spencer, B. F., Sain, M. K., and Carlson, J. D., "Modeling and Control of Magnetorheological Dampers for Seismic Response Reduction," *Smart Materials and Structures*, Vol. 5, No. 5, 1996, pp. 565-575.
- ¹²Ervin, R. D., Lou, Z., Filisko, F. E., and Winkler, C. B., "Electrorheology for Smart Landing Gear," NASA CR-2000883 (N96-25313), 1996.
- ¹³Lou, Z., Ervin, R. D., Filisko, F. E., and Winkler, C. B., "An Electrorheological Controlled Semi-Active Landing Gear," *Society of Automotive Engineers*, No. 93, 1993, pp. 1403.

- ¹⁴Stanway, R., Sproston, J. L., and El-Wahed, A. K., "Application of Electrorheological Fluids in Vibration Control: A Survey," *Smart Materials and Structures*, Vol. 5, No. 4, 1996, pp. 464-482.
- ¹⁵Wereley, N. M., and Lindler, J. E., "Biviscous Damping Behavior in Electrorheological Dampers," *ASME International Mechanical Engineering Congress and Exhibition: Adaptive Structures and Materials Symposium*, AD-(5)/MD-(87), American Society of Mechanical Engineers, New York, 1999, pp. 67-75.
- ¹⁶Lindler, J. E., and Wereley, N. M., "Parametric Analysis and Testing of Electrorheological Fluid Damper," *Smart Structures and Materials 1999: Smart Structures and Integrated Systems*, edited by Wereley, N. M., *Proceedings of SPIE, Society of Photo-Optical Instrumentation Engineers*, Vol. 3668, Bellingham, WA, 1999, pp. 474-486.
- ¹⁷James, N. A., and Mehdi, A., "Behavior of Magneto-Rheological Fluids Subject to Impact and Shock Loading," *ASME International Mechanical Engineering Congress*, Paper No. IMECE2003-42891, Washington D.C., 2003.
- ¹⁸Browne, A. L., and Johnson, N. L., "Conducting Dynamic Impact Tests Using a "Free-Flight" Drop Tower Facility Part I: Theory," *ASME International Mechanical Engineering Congress and Exposition*, Vol. 1, Paper No. IMECE 2001/AMD-25456, also in *Crashworthiness, Occupant Protection and Bio-Mechanics in Transportation Systems*, ASME Publication AMD-Vol. 251, 2001.
- ¹⁹Johnson, N. L., and Browne, A. L., "Conducting Dynamic Impact Tests Using a "Free-Flight" Drop Tower Facility Part II: Practical Aspects," *ASME International Mechanical Engineering Congress and Exposition*, Vol. 1, Paper No. IMECE 2001/AMD-25459, also in *Crashworthiness, Occupant Protection and Bio-Mechanics in Transportation Systems*, ASME Publication AMD-Vol. 251, 2001.
- ²⁰Browne, A. L., McCleary, J. D., Namuduri, C. S., and Webb, S. R., "Impact Performance of Magnetorheological Fluids," *ASME International Mechanical Engineering Congress and Exposition*, Paper No. IMECE 2004-60542, 2004.
- ²¹Wu, W. P., Zhao, B. Y., Wu, Q., Chen, L. S., Hu, K. A., "The Strengthening Effect of Guar Gum on the Yield Stress of Magnetorheological Fluid," *Smart Materials and Structures*, Vol. 15, 2006, pp. 94-98.
- ²²Choi, Y. T., Wereley, N. M., and Jeon, Y. S., "Semi-active Vibration Isolation Using Magnetorheological Isolators." *AIAA J. Aircraft*, Vol. 42, No. 5, 2005, pp. 1244-1251.
- ²³Kamath, G. M., Hurt, M. K., and Wereley, N. M., "Analysis and Testing of Bingham Plastic Behavior in Semi-Active Electrorheological Fluid Damper," *Smart Materials and Structures*, Vol. 5, No. 5, 1996, pp. 576-590.